AGU PUBLICATIONS

JGR

Journal of Geophysical Research: Oceans

RESEARCH ARTICLE

10.1002/2016JC012595

Salt wedge dynamics lead to enhanced sediment trapping within side embayments in high-energy estuaries

Brian Yellen[1], Jonathan D. Woodruff[1], David K. Ralston[2], D. G. MacDonald[3], and D. S. Jones[4]

[1]Department of Geosciences, University of Massachusetts, Amherst, Massachusetts, USA, [2]Department of Geology and Geophysics, Woods Hole Oceanographic Institution, Woods Hole, Massachusetts, USA, [3]College of Engineering, University of Massachusetts Dartmouth, North Dartmouth, Massachusetts, USA, [4]Geology, Amherst College, Amherst, Massachusetts, USA

Key Points:
- Side embayments are a primary location of long-term sediment trapping in high-energy estuaries
- Sediment trapping is amplified 2–3 times during low discharge when ETM penetrates far enough upstream to encounter embayments with available accommodation space
- SSC introduced by flood-dominated, estuarine-induced circulation is a primary mechanism for off-river sediment trapping

Correspondence to:
B. Yellen,
byellen@umass.edu

Citation:
Yellen, B., J. D. Woodruff, D. K. Ralston, D. G. MacDonald, and D. S. Jones (2017), Salt wedge dynamics lead to enhanced sediment trapping within side embayments in high-energy estuaries, *J. Geophys. Res. Oceans*, *122*, 2226–2242, doi:10.1002/2016JC012595.

Received 28 NOV 2016
Accepted 12 FEB 2017
Accepted article online 15 FEB 2017
Published online 17 MAR 2017

Abstract Off-river coves and embayments provide accommodation space for sediment accumulation, particularly for sandy estuaries where high energy in the main channel prevents significant long-term storage of fine-grained material. Seasonal sediment inputs to Hamburg Cove in the Connecticut River estuary (USA) were monitored to understand the timing and mechanisms for sediment storage there. Unlike in freshwater tidal coves, sediment was primarily trapped here during periods of low discharge, when the salinity intrusion extended upriver to the cove entrance. During periods of low discharge and high sediment accumulation, deposited sediment displayed geochemical signatures consistent with a marine source. Numerical simulations reveal that low discharge conditions provide several important characteristics that maximize sediment trapping. First, these conditions allow the estuarine turbidity maximum (ETM) to be located in the vicinity of the cove entrance, which increases sediment concentrations during flood tide. Second, the saltier water in the main channel can enter the cove as a density current, enhancing near-bed velocities and resuspending sediment, providing an efficient delivery mechanism. Finally, higher salinity water accumulates in the deep basin of the cove, creating a stratified region that becomes decoupled from ebb currents, promoting retention of sediment in the cove. This process of estuarine-enhanced sediment accumulation in off-river coves will likely extend upriver during future sea level rise.

1. Introduction

Understanding how and where sediment is stored within river systems presents one of the most crucial challenges to characterizing long-term sediment inputs to the global ocean [*Milliman and Meade*, 1983; *Milliman and Farnsworth*, 2011]. Estuaries tend to be efficient sediment traps, as density gradients and gravitational circulation promote retention and mud deposition [e.g., *Meade*, 1969; *Geyer et al*., 2001]. However, shallow, energetic estuaries with strong tides and river flow are less retentive of fine sediment, and therefore dominated by sandy bottoms. High flow velocities in the main channel often exceed thresholds for fine-grain sedimentation. While ephemeral sediment trapping can occur at salt wedge fronts, where bottom convergence causes elevated turbidity [*Grabemann and Krause*, 1989; *Geyer and Kineke*, 1995; *Ralston and Stacey*, 2007; *Galler and Allison*, 2008], this material is often scoured and redistributed by tidal bed stresses [*Woodruff et al*., 2001] or exported to the ocean by subsequent high discharge [*Galler and Allison*, 2008]. Consequently, the main stems of energetic estuaries tend to have sandy beds and low rates of sediment accumulation [e.g., *Horne and Patton*, 1989]. Outside the main channel, side embayments and off-river coves provide lower energy environments that have the vertical accommodation space necessary to store sediments long term and reduce net sediment delivery to the ocean. The role of such marginal coves in the sediment budget of energetic estuaries and associated sediment transport processes remains relatively unexplored.

Within the tidal freshwater reaches of rivers, *Woodruff et al*. [2013] showed that off-river coves play an outsize role in trapping sediment. These coves can form by channel meander and braid cutoffs and by drowning of fluvial or glacial valleys during rising sea level. They are common along the coastlines of passive margins where low-gradient rivers can have tidal reaches of 50–1000 km including the Amazon River [*Kosuth et al*., 2009], Mekong River [*Nowacki et al*., 2015], Fitzroy River [*Bostock et al*., 2007], and Columbia River [*Jay et al*., 2015]. Tie channels connect coves to the main river channel and may persist naturally due

to tidal flushing or be actively maintained by activities such as dredging or wood removal. These coves accumulate sediments from the river in proportion to tidal range and suspended sediment concentration (SSC) in the river [*Woodruff et al*., 2013].

Relative to nontidal oxbows and coves, tidal freshwater coves accumulate sediment at much greater rates due to flood tide-dominated pumping of suspended sediments into these settings [*Woodruff et al*., 2013]. The greatest sediment input to these tidal freshwater coves is during periods of moderate-to-high discharge, which provide substantial river-derived SSC while still allowing tides to propagate upstream. However, when located within the salinity reach, sediment trapping in off-river coves may also be influenced by estuarine processes. For example, in many estuaries, the region with the highest suspended sediment concentrations, or estuarine turbidity maximum (ETM), is found near the landward limit of the salinity intrusion [*Postma*, 1967], where flow convergence [*Postma*, 1967; *Festa and Hansen*, 1978] and spatial gradients in stratification [*Geyer*, 1993] promote retention and accumulation of fine sediment. The increased sediment concentrations due to these trapping processes can lead to increased deposition of fine sediments near the salinity limit, and thus more fine bed material available for resuspension by tidal currents [*Wellershaus*, 1981; *Grabemann and Krause*, 1989]. Because the length of the salinity intrusion in an estuary varies inversely with freshwater discharge [*Hansen and Rattray*, 1965; *Prandle*, 1981; *Monismith et al*., 2002], the location of the ETM and the zone of fine sediment deposition can vary seasonally depending on river flow [*Ralston et al*., 2012].

The hydrodynamic processes associated with the ETM makes many estuaries efficient traps of fine sediment, leading to channel infilling and muddy bed composition [*Meade*, 1969]. However, tidal salt wedge estuaries have energetic tidal and river velocities and relatively short salinity intrusion lengths that result in less fine-grained accumulation within the main channel and a more sandy bed. Examples include the Fraser River [*Milliman*, 1980], Columbia River [*Gelfenbaum*, 1983], and Skagit River [*Ralston et al*., 2013] in western North America and the Connecticut River [*Horne and Patton*, 1989] and Merrimack River [*FitzGerald et al*., 2002] in the northeast U.S. In the Connecticut, primarily ebb-oriented sand waves have been interpreted as indicating a net seaward movement of sands via bed load transport [*Horne and Patton*, 1989]. The main channel is predominantly sandy with little accumulation of fine-grained sediments. However, roughly 17% of fine-grained sediment transported to the tidal reach of the Connecticut River is stored within that reach [*Patton and Horne*, 1992], hypothesized to be trapped largely in mud-dominated environments that fringe the main channel. Deeper side embayments connected to the main channel provide additional sheltered, lower energy settings with significant accommodation space for the long-term accumulation of fine-grain sediments [e.g., *Woodruff et al*., 2013]. The mechanisms for trapping and accumulation of fine sediments in these coves that reside within energetic salt wedge estuaries have not been investigated and are the focus of this study.

Here we present a detailed assessment of seasonal deposition rates and characteristics of accumulated sediment in Hamburg Cove, a side embayment to the Connecticut River estuary. Geochemical signatures of fresh versus marine sediments are employed to provide an explanation of seasonal sediment sourcing. We couple these observations with hydrographic observations and numerical simulations of sediment and salt transport in order to assess the importance of estuarine processes in trapping sediments in off-channel side embayments.

2. Site Description

Hamburg Cove (41.375, −72.363) is a drowned, glacially scoured bedrock basin located approximately 14 km from the mouth of the Connecticut River (Figure 1). A 30 m wide, ∼3.5 m deep maintained navigation channel cuts through a ∼200 m wide, shallow (<1 m) sill that separates the deepest part of the cove (>5 m) from the Connecticut River. The site is located in the oligohaline portion of the estuary [*Odum*, 1988] just seaward of the extent of salt intrusion during low discharge conditions [*Patton and Horne*, 1992]. Modern fine-grained sedimentation rates within the deepest sections of Hamburg Cove of 4.2 cm/yr [*Woodruff et al*., 2013] are roughly 16 times the average rate of sea level rise since 1940 (2.55 mm/yr) [*NOAA*, 2016]. However, it has been unclear whether this sediment is introduced primarily during moderate-to-high river discharge events, when suspended sediment concentrations in the river are greatest and the cove is

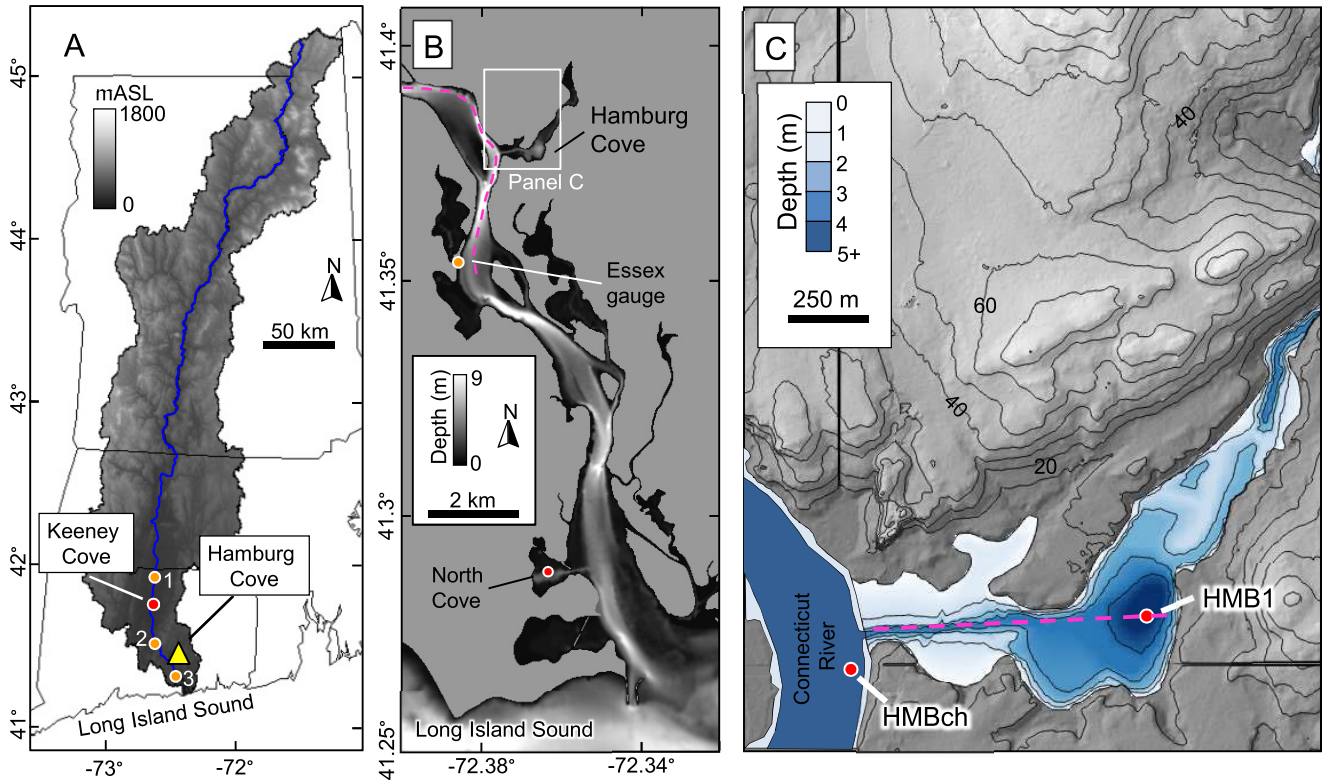

Figure 1. (a) Connecticut River watershed with locations of Hamburg Cove (triangle), Keeney Cove (red circle), and relevant USGS gauges: 1 = Thomsponville, CT; 2 = Middle Haddam, CT; 3 = Essex, CT. (b) Connecticut River estuary bathymetry with precise location of Hamburg Cove and North Cove sediment trap. (c) Hamburg Cove bathymetry and surrounding terrain with 20 m contour intervals. Red circles indicate mooring locations. Pink dashed lines indicate model domains depicted in Figure 10.

fresh [*Woodruff et al*., 2013], or during low river discharge when the salinity intrusion extends to the mouth of the cove and estuarine-induced, upriver transport is enhanced [*Ralston et al*., 2017].

The Connecticut River watershed spans roughly 29,000 km^2 and is the longest river in the northeastern United States. Precipitation is distributed evenly throughout the year [*Magilligan and Graber*, 1996], with snowmelt and vegetation-driven changes in soil moisture controlling seasonal discharge patterns. Mean annual discharge (Q) is about 500 m^3/s. Low discharge of 140 m^3/s or less occurs 10% of the time, generally in the late summer (lowest median daily Q is 10 September). High discharge occurs during spring snow melt, with median daily discharge exceeding 1000 m^3/s throughout April, resulting in a median center of mass date of 6 May. Above the river's tidal limit, suspended sediment concentration scales with discharge according to a power law relationship [*Patton and Horne*, 1992; *Woodruff et al*., 2013], resulting in the majority of sediment delivery to the estuary during seasonal high discharge in March–May. *Patton and Horne* [1992] estimated an average annual fine-grained sediment load of 760,000 t/yr. However, sediment export during rare late-season hurricane-induced floods can exceed annual sediment loads in just a few days [*Yellen et al*., 2014].

The mean tidal range at Essex, CT (see Figure 1) is 1.1 m, and tidal stage changes propagate roughly 100 km inland. Tidal velocities in the estuary approach 1 m/s [*Ralston et al*., 2017]. During moderate-to-high discharge, the Connecticut estuary is a tidal salt wedge, with a stratified, frontal salinity intrusion propagating tidally 5–10 km from the mouth [*Ralston et al*., 2017]. Under low discharge conditions, the estuary tends to be more partially mixed and the salinity intrusion can extend 15 km or more from the river mouth [*Horne and Patton*, 1989].

3. Data Collection

Field observations for this study spanned high and low discharge conditions during spring through fall of 2014, as well as one month of initial observations during low discharge conditions in late summer of 2013.

A U.S. Geological Survey (USGS) gauge at Thompsonville, CT (gauge 01184000, Figure 1), located 93 km upstream of Hamburg Cove provides measurements of freshwater discharge upstream of tides, capturing inputs from 86% of the Connecticut River watershed. Discrete, depth-averaged SSC measurements for various discharges at Thompsonville were used to create a rating curve between discharge and SSC [*Woodruff et al*., 2013] and sediment load [*Yellen et al*., 2014]. An additional USGS gauge 26 km upstream from Hamburg Cove at Middle Haddam, CT (gauge 01193050, Figure 1a), provides continuous measurements of tidal stage and near-surface turbidity, which has been correlated to SSC [*Yellen et al*., 2014]. A multisensor gauge in the upper estuary at Essex, CT (USGS gauge 01194750, Figure 1b), 4 km downstream of the Hamburg site, provides observations of tidal stage, near-surface turbidity, salinity, and temperature.

In the deep basin of Hamburg Cove (HMB1, Figure 1c), sediment traps were recovered and redeployed roughly monthly over the study duration. Data loggers installed at HMB1 and in the main stem of the Connecticut near the entrance to Hamburg Cove (HMBch, Figure 1c) recorded near-bottom conductivity, temperature, and stage at 1 or 5 min intervals throughout most of the sediment trap deployments. A Nortek Aquadopp Acoustic Doppler Current Profiler (ADCP) at HMB1 recorded water column velocities averaged over 5 min intervals, with backscatter intensity used as a proxy for SSC [e.g., *Wall et al*., 2006].

Sediment traps consisted of three cylindrical funnels 11 cm in diameter and 25 cm from rim to spout with a collection tube attached to each spout. A compromise was sought between a longer cylinder, which minimizes biasing [*Butman*, 1986; *Barker et al*., 1988] and proximity to the cove bottom in order to sample the entire overlying water column. Each funnel was mounted spout-down onto a rigid 0.5 m long polyvinyl chloride pipe, which was threaded onto a line and moored with the funnel openings roughly 0.7 m above the cove bottom. At the time of each sediment trap servicing a sediment core approximately 30 cm in length was collected at HMB1 with a Uwitek gravity corer. The top 5 cm of each core was subsampled in the lab at 0.5 cm resolution.

Of the three funnels in each deployment, the collection vial with intermediate accumulation was selected and all of the material was dried and weighed to assess accumulation in g/cm^2. The other two samples were archived for future study. Following measurement of beryllium-7 activity (described below), samples were prepared for grain size analysis following procedures in *Parris et al*. [2009] and analyzed with a Coulter LS200 laser diffraction particle size analyzer.

Beryllium-7 (^{7}Be) is a cosmogenic isotope that has been used to identify recent deposition in estuarine and shelf environments [*Olsen et al*., 1986; *Sommerfield et al*., 1999; *Palinkas et al*., 2005]. Its prevalence in meteoric water, strong tendency to sorb to suspended fines, and its short half-life of only 53.3 days make it a useful proxy for recent deposition. ^{7}Be activity in sediment samples was measured with a Canberra GL2020R low energy germanium detector. Monthly sediment trap samples were used to assess variability in ^{7}Be delivery to the estuary. Depth of detectable ^{7}Be in sediment cores was measured to evaluate monthly deposition independently from sediment trap accumulation observations [*Palinkas et al*., 2005].

Stable carbon isotope ratios of bulk organic material have been applied widely to tag sediment source in various coastal environments, with less negative δ^{13}C values corresponding to marine organics [*Haines*, 1976; *Thornton and McManus*, 1994; *Lamb et al*., 2006]. Representative marine and freshwater end-member sediment samples were collected to evaluate this assumption. Stable carbon isotope ratios (δ^{13}C) and total organic carbon content within sediment trap samples were measured to evaluate marine versus freshwater provenance. Dried and homogenized sediment was combusted in a Costech ECS 4010 Elemental Analyzer, and the evolved CO_2 was analyzed for δ^{13}C using a Picarro G2201-I cavity ring-down spectrometer. Samples were calibrated to USGS-40 and IAEA-CH6 reference standards, and precision was monitored using an in-house acetanilide standard. Isotope ratios are reported relative to the VPDB scale with a precision of 0.1‰.

Freshwater sediment samples were collected with a sediment trap and 30 cm core in July 2015 at Keeney Cove, located 30 km downstream of the head of tides and approximately 55 km upstream of the maximum salinity intrusion (Figure 1a). Suspended sediments advect tidally into Keeney Cove via a tie channel, resulting in rapid rates of accumulation on the order of 3 cm/yr [*Yellen et al*., 2016]. The marine end-member site, North Cove is an actively dredged federal harbor 2.5 km from the Connecticut River mouth that contains salt at all but the highest discharge levels (Figure 1b). Dredging records from 2008 and 2014 indicate modern sedimentation rates of 14 cm yr^{-1} in the maintained harbor, roughly 3 times greater than that at

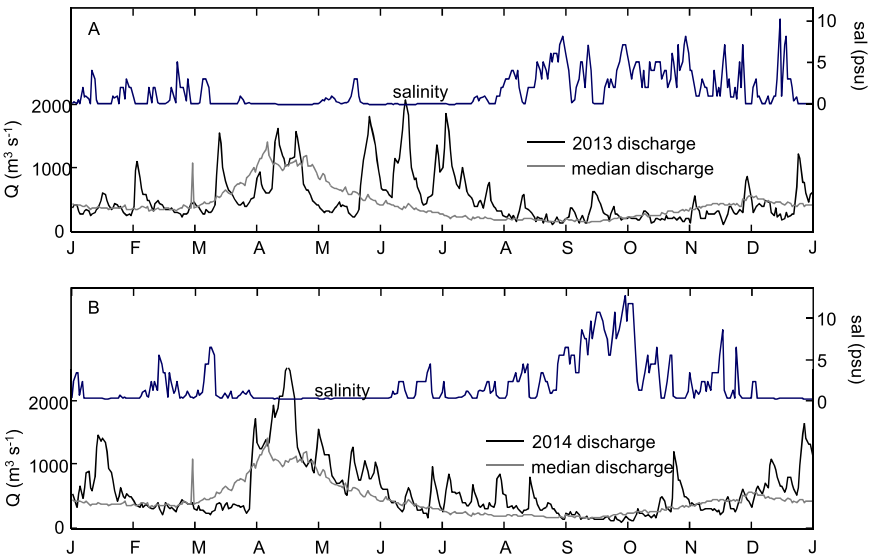

Figure 2. Mean daily salinity and discharge conditions for the Connecticut River across (a) 2013 and (b) 2014. Salinity observations from near surface at Essex, CT, 4 km downstream of HMB1. Discharge observations from above the head of tides at Thompsonville, CT.

Hamburg Cove. A sediment trap was deployed in North Cove during July 2015 and a sediment core was collected there in October 2015 to evaluate late season changes in ^{7}Be and δ^{13}C.

Hydrologic conditions during September 2013 were typical of late summer low discharge (Figure 2). During the April–October 2014 field season, discharge was slightly elevated above long-term averages. Discharge generally decreased throughout the growing seasons of 2013 and 2014, with characteristically low values during September of both years. In the upper estuary at Essex, 4 km downstream of Hamburg Cove (Figure 1b for location), near-surface salinity was low or undetectable from March, 2014 through July, but reached 5–10 psu from July onward as freshwater discharge decreased (Figure 2b).

Cumulative annual discharge in 2014 fell in the 69th percentile of years since 1970, with discharge exceeding long-term median daily discharge throughout much of April–August (Figure 2B). The 2014 spring freshet was typical, peaking at 2600 m^3/s, 5% above the long-term median peak discharge for March–May. Estimated sediment discharge above the head of tides based on freshwater discharge and a rating curve from *Woodruff et al.* [2013] was 550 kt, roughly equivalent to the rating curve-derived long-term average (mean = 590 kt, median = 530 kt). Of the total sediment load in 2014, 56% was delivered to the tidal river between 15 April and 15 May.

In order to obtain a better spatial distribution of data, an IVER2 (OceanServer, Fall River, MA) autonomous underwater vehicle (AUV) was deployed to collect water column measurements of salinity, temperature, and turbidity on 14 September 2014. The instrument orients itself underwater using paired ADCP units and surfaces at preprogrammed waypoints to correct course using GPS. The AUV made repeated circuits every 15 min around the deep section of Hamburg Cove through one tidal cycle, alternating its route between near surface and 1 m above bottom.

4. Model Design

We used a numerical model to examine how hydrodynamic processes in the estuary influence sediment accumulation rates observed in Hamburg Cove. To compare model results directly with the sediment trap observations, accumulation rates are calculated as the cumulative sediment flux into Hamburg Cove divided by the cove's deep area (>3 m) and the duration of each simulation.

A hydrodynamic and sediment transport model of the Connecticut River was developed using the Finite Volume Community Ocean Model (FVCOM) [*Chen et al.*, 2003]. FVCOM solves the Reynolds-averaged Navier-Stokes equations for mass and momentum on an unstructured grid with terrain-following coordinates vertically. The Community Sediment Transport Modeling System (CSTMS) [*Warner et al.*, 2008] has been

incorporated into FVCOM to simulate sediment transport, including suspended sediment fluxes and a multilayer bed model. FVCOM with CSTMS has been used previously to model sediment transport for the Skagit River, another shallow, energetic salt wedge estuary with a mixed grain size distribution [*Ralston et al.*, 2013].

The details of the model development and validation for the Connecticut River estuary model are described elsewhere [*Ralston et al.*, 2017], with an overview of key components provided here. The model domain includes all of Long Island Sound and extends up to the tidal limit of the Connecticut River. Grid resolution is greatest in the estuary region from the mouth of the Connecticut up to Hamburg Cove, with typical horizontal grid spacing of 15–20 m. The vertical grid was terrain following with 30 uniformly spaced sigma layers. The model has been extensively evaluated against time series of water level, velocity, salinity, and suspended sediment concentration and found to be largely consistent with observations [*Ralston et al.*, 2017]. A detailed comparison of model results against high spatial and temporal resolution field surveys found that a fine grid resolution was necessary to mitigate numerical mixing and simulate the strong stratification and sharp horizontal salinity gradients. Fine sediment trapping in the estuary was largely driven by enhanced stratification and reduced bed stress at bottom salinity fronts, most notably in regions of bathymetric transitions.

The model was forced with observed river discharge at Thompsonville, tidal water levels at the western and eastern ends of Long Island Sound (NOAA stations at Newport, RI, #8452660; Montauk, NY, #8510560; and Kings Point, NY, #8516945), and wind extracted from the North American Mesoscale (NAM) Forecast System 12 km resolution model. Suspended sediment was simulated using three representative size classes based on the observed bed sediment composition: fine-to-medium sand (~250 μm) with settling velocity (w_s) = 30 mm s^{-1}, coarse silt (~60 μm) with w_s = 3 mm s^{-1}, and fine-to-medium silt (~20 μm) with w_s = 0.5 mm s^{-1}. Suspended sediment discharge from the Connecticut River is based on the rating curve at Thompsonville [*Woodruff et al.*, 2013], split 40/60% between the finer sediment classes. The bed sediment distribution was based on a quasi-equilibrium state after initializing with a uniform distribution and then allowing the model to run and redistribute sediment for an extended period (>1 month). The model captured seasonal trends in the bed sediment composition, with less fine sediment in the estuary during the high discharge of the spring freshet and more fine sediment during moderate and low discharge periods.

Here we use results from realistic simulations that correspond with periods of observation in the estuary for model validation, and some of which overlap with the sediment trap deployments in Hamburg Cove. The realistic simulations span a range of river discharge conditions, including high discharge, spring freshet (May 2014, $Q_{r,avg}$ = 980 m^3 s^{-1}), moderate discharge fall (November 2013, $Q_{r,avg}$ = 320 m^3 s^{-1}), and low discharge late summer (August 2013, $Q_{r,avg}$ = 190 m^3 $s^{-1}$and September 2014, $Q_{r,avg}$ = 160 m^3 s^{-1}). Each case was run for approximately 3 weeks after an initial spin-up period of several days.

5. Results

5.1. Water Column Observations

At Hamburg Cove, water column data reveal similar seasonal salinity patterns to those observed just downstream at Essex (Figure 3). During 2014, saline estuarine water arrived at the entrance to Hamburg Cove (HMBch) by mid-June and salinities generally increased during August–October (Figure 3b). Persistent salinity intrusion into the cove at HMB1 lagged several weeks behind the arrival of salinity in the main channel of the river near the entrance to the cove (Figure 3c). Temporal variability of salinity from Hamburg Cove's internal basin contrasted with those from the sensor in the Connecticut River's main channel at the entrance to the cove. Whereas main channel salinity varied with tidal advection of the salinity intrusion, salinity in the bottom water of Hamburg Cove rose abruptly and then slowly decayed to lower levels over several days (Figure 4a), despite continual tidal fluctuations in water level in the cove. Sharp increases in near-bottom salinity in the cove corresponded with pulses of near-bottom, landward flow at the HMB1 mooring of 5–10 cm/s (Figure 4b), as well as increased acoustic backscatter (Figure 4c). During most of the deployment period, near-bottom velocities were much lower (<3 cm/s).

Continuous turbidity measurements at the Essex, CT USGS gauge illustrate the relationship among river discharge, salinity, and sediment availability in the upper estuary. During November–July, when freshwater discharge tends to be greater than or equal to the median annual flow, maximum daily turbidity displayed a

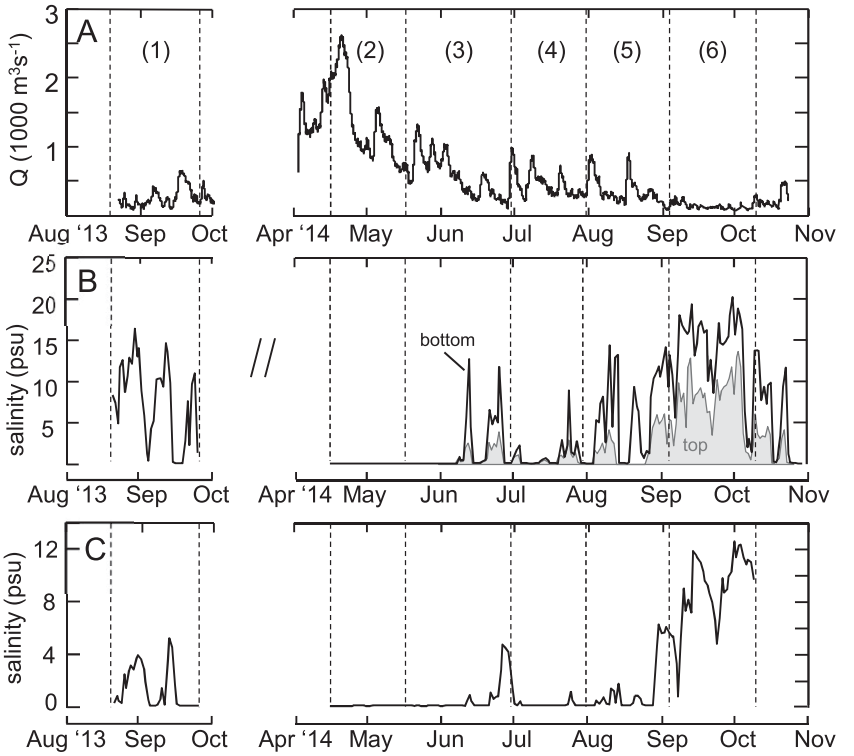

Figure 3. Water column observations spanning the 2013–2014 monitoring periods. Dashed vertical lines indicate sediment trap deployment durations, with numeric labels referenced in Table 1. (a) Freshwater discharge at Thompsonville, CT. (b) Maximum daily salinity in the Connecticut River at the entrance to Hamburg Cove (HMBch location) at the top of the water column (shaded) and bottom (black line) at a mean water depth of 9.7 m. (c) Bottom (mean depth of 5.4 m) salinity averaged daily in Hamburg Cove (HMB1 location).

positive power law relationship with discharge (Figure 5a), as has been noted above the tidal limit at Thompsonville, CT [*Patton and Horne*, 1992; *Woodruff et al*., 2013]. However, during low discharge periods (August–October), turbidity in the upper estuary increases despite minimal sediment inputs from the watershed during this time. Separating these data into times when salinity was present or absent at the gauge shows that the highest turbidity readings occur during times when salinity is observed at the Essex gauge (Figure 5b).

To evaluate the timing of SSC availability with respect to the tidal cycle during low river discharge, maximum daily turbidity at Essex was plotted against tidal hour for each day during the September 2014 deployment (Figure 5c). Tidal phase was calculated from water surface elevation, with the flood starting 1.5 h after low water to account for the phase lag of velocity for the partially progressive tide. Nearly all daily turbidity peaks occurred midway during the flood tide, with an average tidal hour of 3.9 for turbidity observations that exceeded 50 ntu. Turbidity tended to be greater during periods with salt present; 75% of observations greater than 50 ntu occurred when bottom salinity exceeded 8 psu.

5.2. Sediment Trap Accumulation

Sediment accumulation in Hamburg Cove traps during the 2014 field season totaled 0.92 g cm^{-2}. The deep section of the cove (>3 m) has a spatial extent of 0.13 km^2, comprising roughly 0.2% of the total area of the tidal river and estuary (Figure 1). Extending HMB1 deposition rates in 2014 over just this deeper area yields a total of 12 kt yr^{-1}, or 0.9% of the tidal river's annual sediment storage [*Patton and Horne*, 1992]. Using a porosity of 0.85 for surficial sediments at HMB1 [*Kratz*, 2013], this observed mass accumulation equated to a linear deposition rate of 4.8 cm yr^{-1}, which is consistent with a twentieth century rate of 4.2 cm yr^{-1} [*Woodruff et al*., 2013] after considering compaction.

Monthly sediment accumulation rates varied considerably over the deployment period (Figure 6). The two lowest rates of accumulation occurred during the 2014 spring freshet in May and June with rates of 0.14 g cm^{-2} $month^{-1}$ and 0.11 g cm^{-2} $month^{-1}$, respectively. In contrast, the two highest rates of accumulation

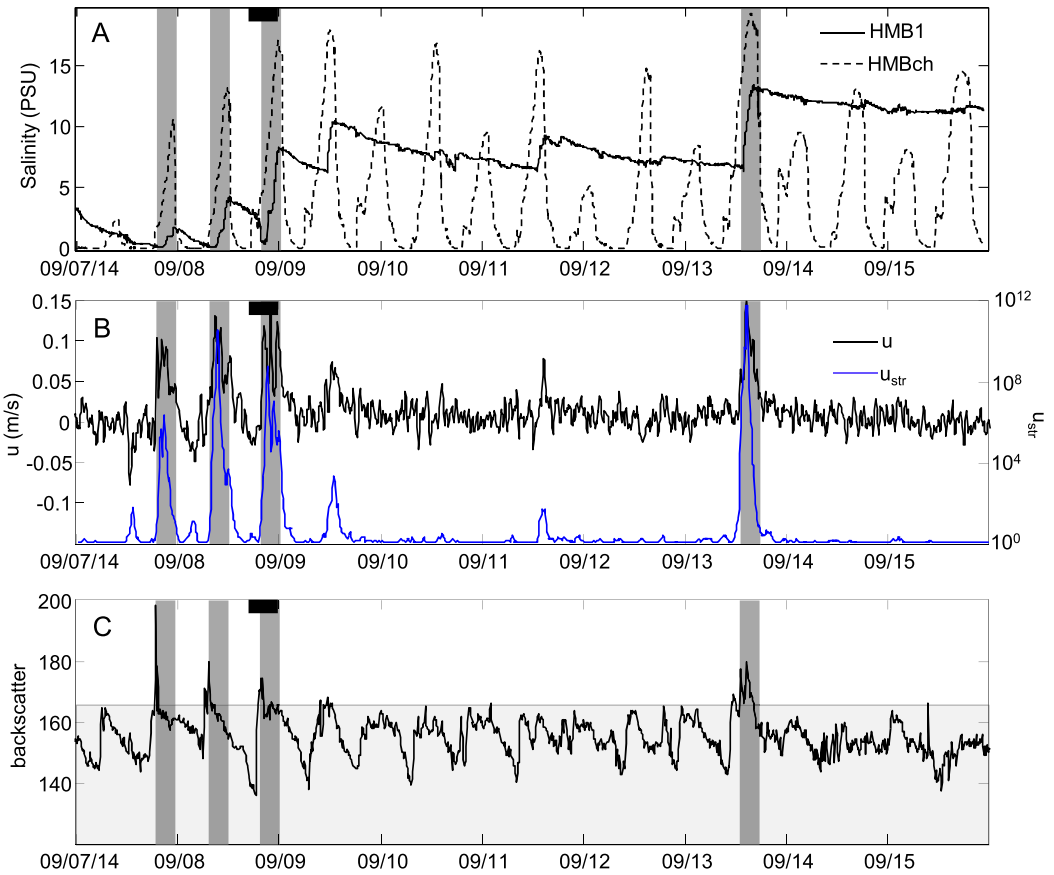

Figure 4. (a) Bottom salinity inside and outside Hamburg Cove (see Figure 1 for locations). (b) Water velocity averaged over the bottom 1 m of the water column at HMB1 (blue) and bottom shear stress proxy, u_{str} ($C_d u_{bot}^2$, C_d = 3E-3). (c) ADCP backscatter intensity at HMB1 averaged over the bottom 1 m at HMB1. Bold black bars at top of each figure indicate timing of model run in Figure 11 (m) and autonomous underwater vehicle (AUV) transects in Figure 12.

occurred during the two lowest discharge months in the study, September in 2013 and 2014 (Figure 2, Table 1). Sedimentation rates during these low discharge months were 0.36 and 0.23 g cm^{-2} $month^{-1}$, roughly 100–200% higher than during the spring freshet of 2014. Median grain size within sediment trap samples averaged 16 μm, with little variation between deployments (Table 1).

River water column variables such as discharge and turbidity were averaged across individual trap deployment durations to evaluate possible correlations with sediment accumulation. Although the sample size (n = 6) is too small for robust statistical analysis, Pearson's r-values and corresponding *p*-values were calculated for comparison between independent variables. Sediment accumulation correlated poorly with turbidity at Middle Haddam (r = 0.34, $p = 0.51$), which provides a reliable proxy for direct sediment supply from the watershed (Figure 7a). A similar weak correlation was observed with turbidity observations from the upper estuary at Essex (r = −0.23, $p = 0.66$), where we have shown that high turbidity can be decoupled from discharge during periods with low discharge and increased salinity (e.g., Figure 5). Therefore, in terms of a direct correlation neither sediment supply from the upper watershed nor suspended sediment concentrations in the estuarine water column at Essex is the dominant factor controlling sediment accumulation rates in Hamburg Cove. Of water column observations evaluated, only discharge displayed a moderate inverse correlation with sediment accumulation (Figure 7b).

5.3. Sediment Trap Geochemistry

Samples collected from fresh and seaward end-members (Keeney Cove and North Cove, respectively) revealed clear geochemical differences in sediment composition. $\delta^{13}C$ was −29.1‰ for the freshwater cove, compared to −24.5‰ for the marine cove at the mouth of the estuary during both high and low discharge conditions. Observations are consistent with consensus $\delta^{13}C$ values for marine organic content ranging

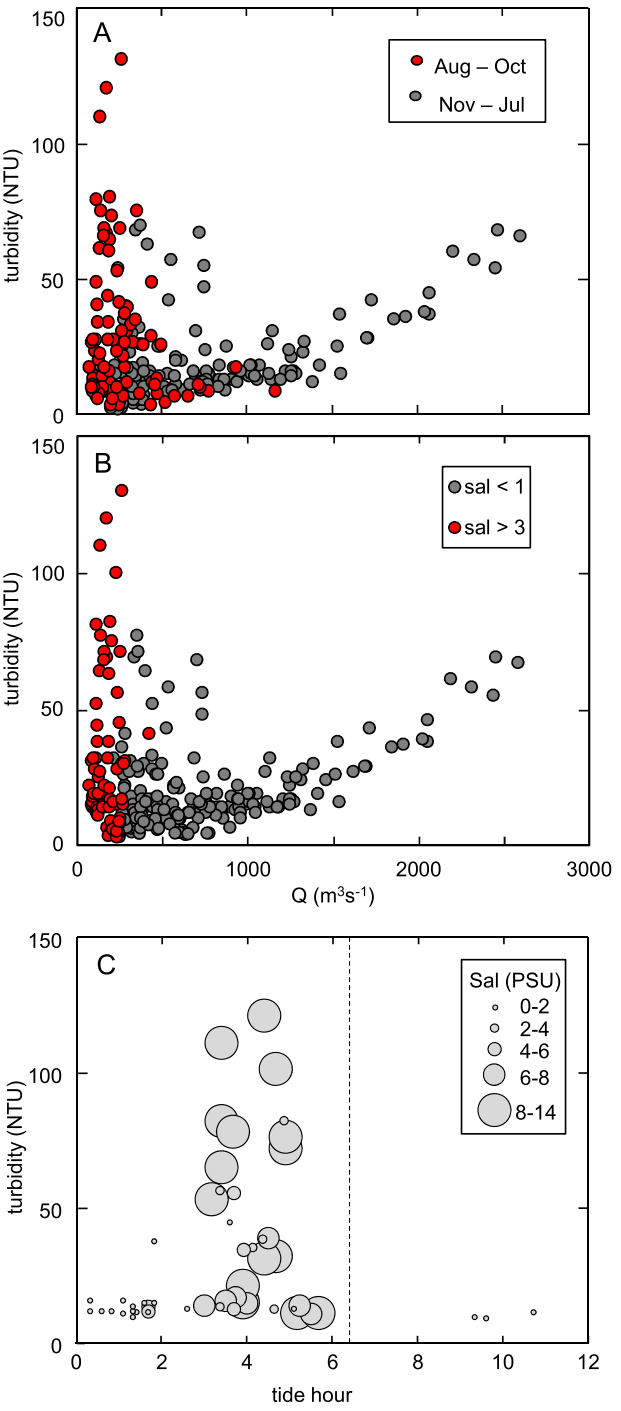

Figure 5. Maximum daily turbidity in the upper estuary at Essex (USGS gauge 1194750) plotted as a function of discharge: (a) data points grouped by season; (b) data points grouped by bottom salinity at Essex. (c) Maximum daily turbidity during September 2014 sediment trap deployment as a function of tidal hour, where high tide ≈ 6.25 h (dashed line). Bottom salinity indicated by marker size.

from −16‰ to −24‰, compared to −25‰ to −33‰ for terrestrial C3 plant particulate matter, and −25‰ to −30‰ for freshwater algae [*Lamb et al.*, 2006]. Within monthly sediment traps at HMB1, the highest $\delta^{13}C$ (least depleted) values were observed during two September deployments, which corresponded to the lowest monthly discharge values and highest salinities in the cove (Table 1). Conversely, the lowest $\delta^{13}C$ value of −28.7‰ occurred during the deployment of second highest average discharge and closely followed the spring freshet. Thus, late season, low discharge periods coincided with the most marine $\delta^{13}C$ values for accumulated sediment and highest salinities in the cove. In general, there was an inverse relationship between $\delta^{13}C$ and mass accumulation rates in Hamburg Cove (Figure 7c).

Using $\delta^{13}C$ values from North Cove and Keeney Cove sediment traps as estuarine and freshwater end-members, respectively, we applied a linear end-member mixing model to approximate the percentage of material from the estuary that was trapped in Hamburg Cove [*Hedges and Parker*, 1976].

$$OC_{marine}(\text{fraction}) = 1 - \frac{\delta^{13}C_{sample} - \delta^{13}C_{marine}}{\delta^{13}C_{terr} - \delta^{13}C_{marine}}$$

September sediment corresponding to low river discharge and maximum accumulation in 2013 and 2014 contained 56% and 44% marine-sourced organic matter, respectively. May–August trap material averaged 26%, with a minimum of 6% marine-sourced organic matter following the spring freshet (Table 1).

5.4. ^{7}Be Variability and Down-Core Profiles

As observed with $\delta^{13}C$ values, ^{7}Be activities indicated distinct source material for freshwater and marine end-member sites. Sediment trap ^{7}Be concentrations upstream at the freshwater Keeney Cove site were nearly 3 times greater than near the mouth of the estuary at North Cove during the month of July 2015 (Figure 8a), despite sedimentation rates in North Cove being over 4 times greater than in Keeney Cove. By October 2015, following prolonged low discharge conditions and elevated salinity at North Cove, ^{7}Be was undetectable in the top 0.5 cm of a sediment core collected there. High deposition rates in North Cove and low-to-undetectable ^{7}Be activities support a depletion of ^{7}Be in the marine derived sediments that primarily accumulate in the cove.

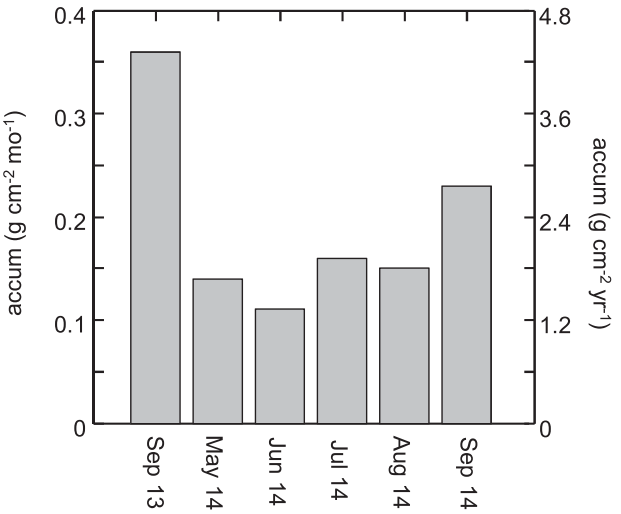

Figure 6. Sediment accumulation in monthly sediment traps at HMB1.

Monthly sediment trap samples at HMB1 revealed relatively constant ^{7}Be sourcing, with the exception of the September 2014 sample, which was somewhat lower and similar to that observed in North Cove July sediments (Figure 8a). The activity of ^{7}Be in surface sediments at HMB1 from recovered cores provided a useful measure of monthly sediment deposition independent of sediment trap estimates (shown as circles in Figure 8a). ^{7}Be values in the top half centimeter of sediment cores increased throughout 2014 observations, echoing sediment trap observations of higher accumulation during late summer (Figures 8a and 8b). Furthermore, low total ^{7}Be inventories in the April core (Figure 8b) suggest minimal deposition during winter months when we did not directly monitor deposition with sediment traps.

Relatively constant ^{7}Be activity in sediment trap samples at HMB1 (Figure 8a) suggests stable initial ^{7}Be concentrations at Hamburg Cove. Therefore, observed increases in core top ^{7}Be activity (Figure 8b) can largely be attributed to faster deposition and younger sediments in the 0–0.5 cm core subsample, rather than an increase in ^{7}Be activities for sediment at the time of initial deposition. High surficial ^{7}Be activities and maximum total detectable depth at HMB1 were observed in September and October of 2014 (Figure 8b), which is consistent with sediment trap data observations for maximum rates of accumulation during months of lowest discharge.

5.5. Model Results and Observations

Modeled sediment fluxes into the cove were broadly consistent with sediment trap observations (Figure 9). Most notably, cumulative sediment fluxes into the cove were greatest during lower discharge conditions (Figure 10). During the lower discharge model runs (August 2013, September 2014), sediment input from the river was negligible and the sediment flux into Hamburg Cove was almost entirely from remobilized

Table 1. Sediment Trap Parameters and Average River Conditions During Each Deployment[a]

	(1) Sep 2013	(2) May 2014	(3) Jun 2014	(4) Jul 2014	(5) Aug 2014	(6) Sep 2014
Deployment dates	8/20 to 9/25	4/16 to 5/13	5/13 to 6/24	6/24 to 7/29	7/29 to 9/5	9/5 to 10/9
Accum (g cm^{-2} month^{-1})	0.36	0.14	0.11	0.16	0.15	0.23
Sed rate (cm month^{-1})[b]	0.96	0.50	0.25	0.44	0.38	0.65
Sed rate (cm yr^{-1})[b]	11.5	6.0	3.0	5.3	4.5	7.8
Avg Q (m^{3} s^{-1})	263	1286	596	448	333	130
Avg sal Essex (psu)	2.0	0.1	0.3	0.5	1.4	5.3
Essex top temp (°C)	22.7	9.9	19.2	25.1	23.8	20.9
Avg tidal range (m)	0.75	0.96	0.96	0.96	0.96	1.03
Avg Essex turb (ntu)	6.9	15.9	6.7	7.1	7.3	9.1
MidHad Turb (ntu)	4.2	20.2	5.6	4.6	3.8	1.8
δ^{13}C (‰)	−26.5	−27.1	−28.7	−27.3	−27.7	−27.0
Fraction marine[c]	0.56	0.41	0.06	0.38	0.28	0.44
TOC (%)	3.31	4.60	5.15	4.72	5.51	4.70
D_{10} (μm)	2.3	1.79	1.92	2.09	1.92	2.1
D_{50} (μm)	19.87	13.06	15.74	16.13	14.77	17.39
D_{90} (μm)	73.64	40.65	49.48	47.84	45.46	60.69
HMBch bot sal	1.84	0.04	0.17	0.28	0.52	3.52
Be-7 trap (Bq g^{-1})		0.29	0.28	0.23	0.26	0.18
Be-7 core top (Bq g^{-1})		0.14	0.17		0.24	0.28

[a]See Figure 1 for locations of Essex, Middle Haddam, and HMBch.
[b]Using porosity = 0.85 from *Kratz* [2013].
[c]From equation (1).

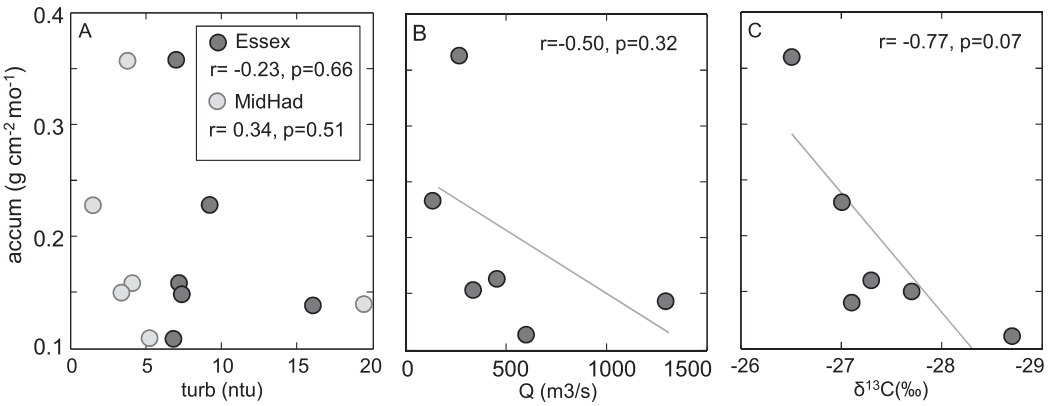

Figure 7. Sediment accumulation plotted as a function various parameters: (a) turbidity in the estuary (Essex) and upstream of salt (Middle Haddam); (b) freshwater discharge at Thompsonville averaged over sediment trap deployment; and (c) $\delta^{13}C$ values of organic material in sediment trap material.

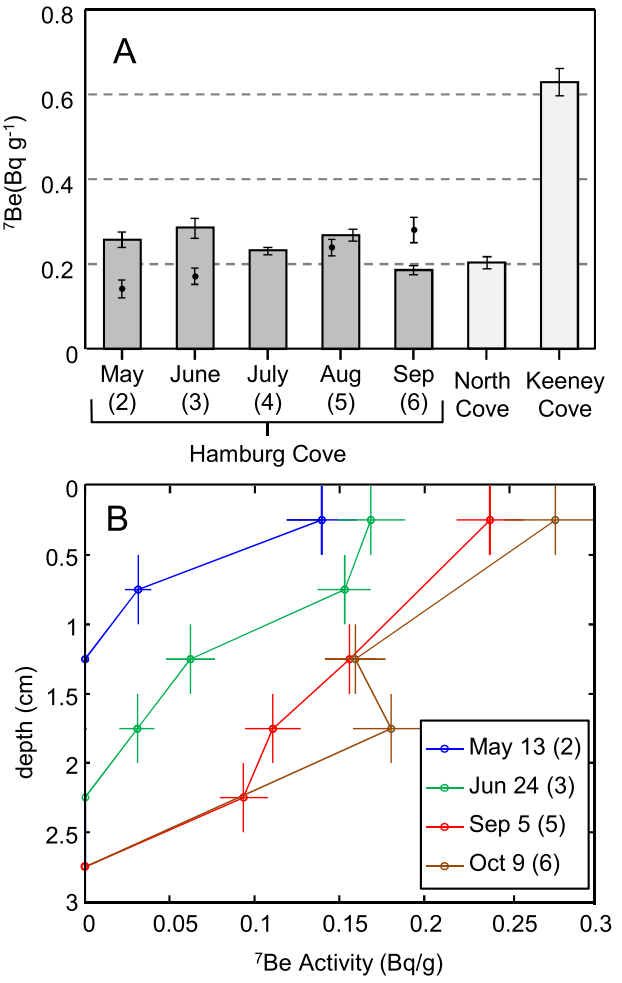

Figure 8. Label numbers correspond to time periods in Table 1. (a) Bar plot of ^{7}Be in 2014 sediment traps from HMB1 and reference sites. Monthly sediment core top (0–0.5 cm) ^{7}Be activities are depicted by black circles. (b) ^{7}Be profiles from short cores collected at HMB1 during 2014. Vertical bars depict sample depth; horizontal bars depict measurement error.

estuarine bed sediment. During the higher discharge simulation period (May 2014), total sediment fluxes into Hamburg were much lower, but much of that was associated with new sediment input from the river. High river flows with the spring freshet also remobilize marine-derived fine-grained bed sediment that was deposited during prior season low discharge conditions. Therefore, the suspended sediment in the estuary is a mix of newer watershed and older estuarine material even during high discharge. Geochemical evidence from trapped Hamburg Cove sediments in May 2014 confirms that significant amounts of marine material and terrigenous material are transported into the cove during the spring freshet. However, following the spring freshet in June 2014, the terrigenous fraction increased, indicating that inputs from the watershed were more dominant (Table 1).

Model results from one tidal cycle during low discharge illustrate the mechanisms by which sedimentation rates in the cove are enhanced by estuarine processes (Figure 11). Water column observations corresponding with the model results are shown in Figure 4. The salinity intrusion moved landward during the flood tide (Figures 11a1−11a3) with weak stratification in the estuary. A local maximum in suspended sediment concentration (or ETM) advected landward with the low salinity region (2–4 psu) near the head of salt. As the salinity

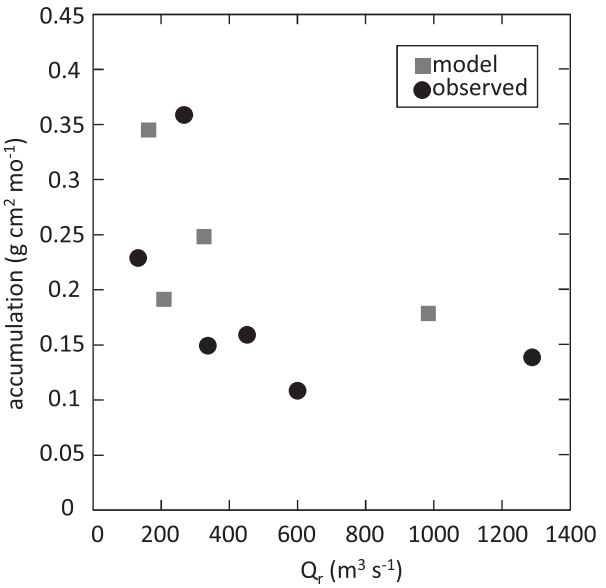

Figure 9. Sediment accumulation rates in Hamburg Cove versus river discharge. Model results are averages over realistic simulations of 2–4 weeks each. Observations are from sediment traps, as in Figure 6a.

intrusion and ETM moved past the entrance to Hamburg Cove, it created a lateral density gradient between the main channel and the interior of the cove (Figure 11b3), which drove a gravity current of saltier water flowing into Hamburg Cove (Figure 11b4). The new pulse of saltier water vertically stratified as it flowed into the cove and the tide slacked, increasing the stratification in the deeper regions (Figures 11b5−11b6).

The suspended sediment in the entrance channel to Hamburg Cove increased initially during the flood due to resuspension by tidal velocities (Figures 11b2 and 11b3), and this material advected into the cove early in the flood. However, much greater suspended sediment concentrations were associated with the ETM and lateral salinity intrusion from the main channel (Figures 11b3 and 11b4). Sediment delivered into the cove with the salinity intrusion initially spread along the pycnocline with the flow (Figure 11b5), and subsequently settled into the deeper basin, below the stratification in salinity. Sediment resuspended by the tidal currents in the entrance channel prior to the lateral salinity intrusion likely was deposited there during prior intrusion events.

Water column data were collected with the AUV on 12 September 2014, 2 days after the model results shown in Figure 11, on a tidal cycle with similar, but slightly weaker salinity fronts (Figure 4a). Turbidity measurements from the AUV are shown in Figure 12. These observations support the pattern of sediment transport into Hamburg Cove suggested by the model and shown in Figure 11. Similar to model runs, AUV turbidity observations suggest an initial burst of sediment entering the cove shortly after low tide, with higher turbidity focused near the channel inlet extending from top to bottom and weakening over several hours. This initial pulse is followed by a secondary pulse at depth shortly after high tide, which progresses from the inlet toward the deepest part of the cove. As discussed above, the first pulse is likely due to the remobilization of channel sediments due to the incoming tide, while the second pulse is associated with the salinity intrusion.

6. Discussion

6.1. Seasonal Geochemical Signatures

As river discharge decreased throughout the monitoring period, accumulated sediment at Hamburg Cove displayed marked changes that reflect a shift toward a more marine influenced sediment source. Decreases in terrigenous fraction in September sediment trap material, as indicated by $\delta^{13}C$, are supported by a similar decrease in ^7Be. This decrease in ^7Be activity is due to reservoir effects of marine water. Because ^7Be is sourced from the atmosphere and decays quickly, it is undetectable in marine sediment, which is relatively disconnected from atmospheric input. This marine water residence effect is reflected in North Cove sediments, where ^7Be activity in surface sediments (0–0.5 cm) was undetectable despite sedimentation rates $>$ 14 cm/yr as indicated by harbor dredge records. Conversely, surface sediments from sediment cores at Hamburg Cove displayed increases in ^7Be activities during low discharge conditions (Figure 7a). Higher ^7Be activities in surface sediments relative to those from concurrent sediment traps (e.g., September 2014) indicate that the average age of deposited sediments in the top half centimeter of the sediment column is less than that of material in the sediment trap. In other words, relative ^7Be concentrations indicate that deposition exceeded 0.5 cm during September 2014.

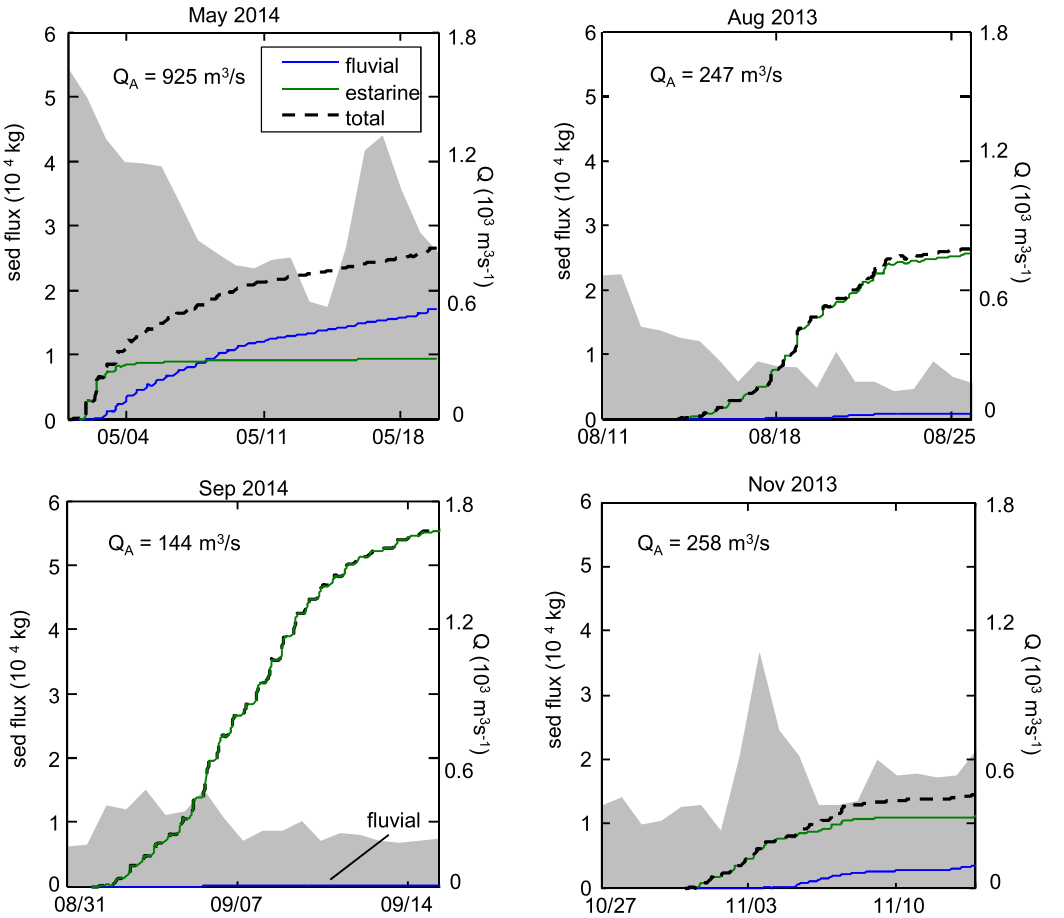

Figure 10. Cumulative sediment flux (dashed line) through the channel entrance to Hamburg Cove for four model runs spanning a variety of discharge conditions. Sediment is distinguished by source, with fluvial sediment (blue line) supplied by freshwater discharge and estuarine sediment (green line) supplied by remobilization of estuarine bed sediment. Daily freshwater discharge at Thompsonville in grey and average discharge for the whole run is reported as Q_A.

6.2. Salinity-Sediment Storage Connections

Weak negative correlation between sediment trap accumulations and river/estuarine turbidity shows that sediment trapping within Hamburg Cove is not driven simply by suspended sediment concentration (Figure 7a). Rather, estuarine dynamics, specifically salt intrusion into the upper estuary, play a key role in driving tidally enhanced sediment trapping in off-river coves. In addition to correlative indications that high salinity and low freshwater discharge drive rapid sediment accumulation at HMB1 (Figures 3–5), geochemical indicators of partially marine-sourced material support the case for estuarine sediment entering the cove during periods of seasonal low discharge.

Observations and model results both suggest that the estuarine turbidity maximum (ETM) play a key role in increased rates of sediment accumulation observed in Hamburg Cove during September deployments. During April–May when discharge was high, sediment concentrations upriver at Middle Haddam were relatively high and yet observed accumulation rates in Hamburg Cove were low, suggesting that most of the river sediment bypasses Hamburg Cove. As discharge decreased toward late summer, the salt wedge and associated ETM migrated landward. By midsummer, the landward limit of salt was located near the entrance to Hamburg Cove as evidenced by oscillating salinity at HMBch (Figure 4a, dashed line). This landward migration of the ETM redistributed sediment from the lower to the upper estuary [*Shubel*, 1968; *Wellershaus*, 1981; *Geyer*, 1993]. Sediment traps collected during low discharge had more marine $\delta^{13}C$ and ^{7}Be signatures, providing evidence that sediment associated with the ETM spent time in marine environments of the estuary and Long Island Sound prior to deposition in Hamburg Cove.

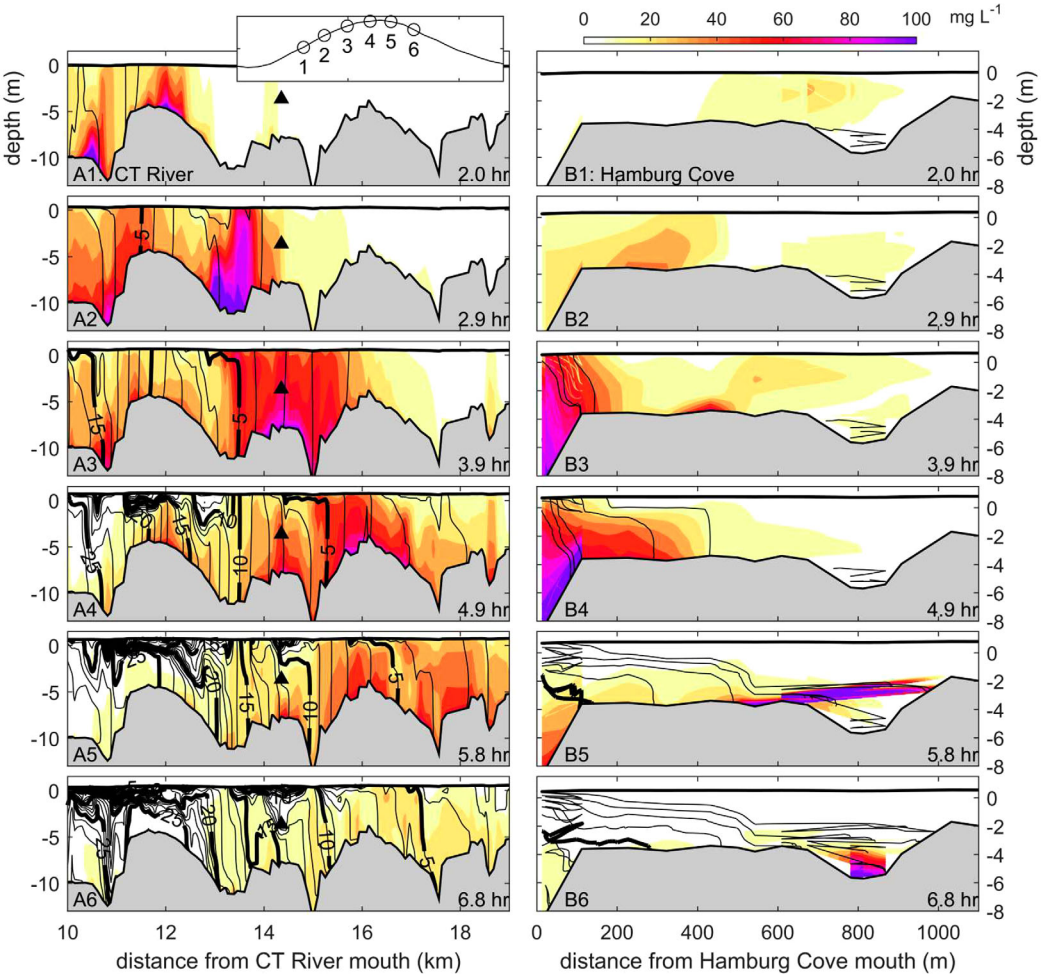

Figure 11. Model results of suspended sediment (color) and salinity (black contours) during a flood tide in September 2014. (top) Timing of figures 1–6 relative to water surface elevation with *y* axis range −1 to 1 m. (left) Along-channel sections in the main stem of the Connecticut River, focusing on a region near the mouth of Hamburg Cove with tidal hour indicated in bottom right of each figure. Location and elevation of channel to Hamburg Cove marked with a triangle. (right) Sections along the channel into Hamburg Cove with time in bottom right of each figure. Salinity contours every 1 psu, with thicker contours every 5 psu. Transect locations are shown in Figure 1.

Sharp increases in salinity and velocity suggest that higher salinity water entered the cove during episodic gravity currents when the pycnocline in the main stem of the Connecticut rose above the sill at the entrance to the cove. The corresponding increase in acoustic backscatter suggests that particulate material was transported into the cove along with the higher salinity water. When the water advecting into Hamburg Cove is saltier than the ambient water in the basin, it tends to plunge as a dense current along the bottom into the deep basin. Further, when previous salinity intrusions give rise to cove stratification, sediment trapping efficiency likely increases as settling particles become trapped in stagnant, dense water below the pycnocline.

6.3. Sediment Transport and Accumulation

Model results provide a mechanistic explanation for high sediment accumulation during low discharge, high salinity conditions in Hamburg Cove. Three factors appear to be contribute to the dramatically amplified sediment storage rates: (1) low discharge conditions allow for the ETM to advance upstream to the upper estuary and make sediment available in the water column for advection into the cove; (2) the lateral salinity gradient between the main stem and the cove creates gravitational currents that advect sediment along the entrance channel and into the deeper parts of the cove; and (3) stratification in the cove facilitates accumulation of sediment by reducing bed stresses and resuspension. The first two factors, the presence of fine sediment in the upper estuary and the lateral transport due to the salinity gradient between

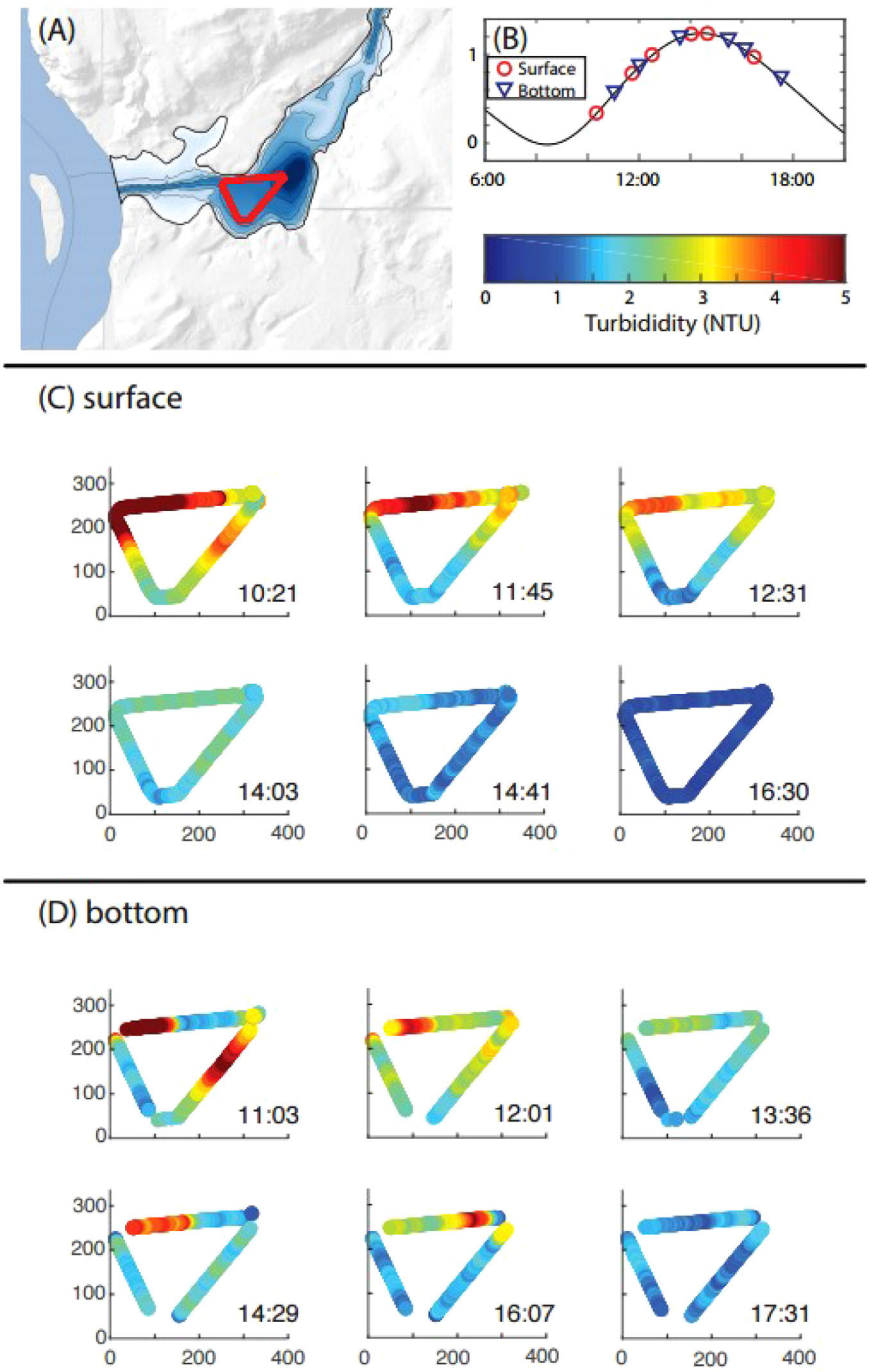

Figure 12. (a) Location of AUV transects on 12 September 2014, as shown by the red line. (b) Transect timing with respect to water level. Red circles and blue triangles represent surface and near-bottom transects shown. (c) Near-surface turbidity with start time indicated. (d) Near-bottom turbidity. Data gaps represent times when AUV surfaced to rectify position.

the main channel and the cove, are dynamically coupled. Estuarine circulation in the main stem brings fine sediment landward during low flow periods. In the entrance channel to Hamburg Cove gravity currents increase bed stress, keeping sediment in suspension as this denser water advects into the cove. The effect of stratification in the deeper parts of the cove on resuspension and export during ebbs may be less important, as the near-bed velocities during periods without stratification remain modest and there is little evidence of resuspension in the acoustic backscatter signal. The weak tidal velocities make the cove a

depositional zone that is highly retentive of sediment advected in from the estuary, and the deeper parts of the cove have sufficient accommodation space to permit the high observed rates of accumulation.

At North Cove, where dredging records indicate very high deposition rates, ongoing accommodation space is only maintained through continual dredging. This suggests that in coves where salinity is present through most discharge conditions, deposition rates are dramatically amplified and coves quickly infill. Given projections for continued sea level rise and increased landward extents of estuarine salinity [e.g., *Temmerman et al*., 2004], coves that are currently tidal freshwater bodies will become influenced by salt and the ETM. This will result in rapid infill by sediment trapping processes similar to those described here for Hamburg Cove. The increase in sediment trapping rates in newly oligohaline coves is likely to impact coastal and estuarine landscapes. At decadal time scales, these coves have the capacity to store sediment at significantly higher rates. At slightly longer time scales, these tidal coves will fill unless accommodation space is maintained by dredging. Given the ecological importance of tidal coves including for fish nursery [*Odum*, 1988] and the societal importance of these features as natural harbors and anchorages, planners and resource managers should be aware of the impermanence of these features.

7. Conclusions

Whereas rivers deliver sediment to estuaries predominantly during high discharge, long-term sediment fine-grained storage in energetic estuaries occurs primarily during periods of seasonal low discharge via tidal advection into off-channel coves. Monthly deposition in sediment traps and geochemical characteristics of the trapped sediment support the crucial role of saline water in the delivery of sediment to these side embayments. As seasonal discharge decreases and the salinity intrusion moves landward, tidally redistributed sediment is suspended and thereby made available for advection out of the main channel and into more depositional coves. Salinity gradients between the main channel and coves drive gravitational currents that enhance lateral sediment transport and create stratification that reduces sediment resuspension in the coves and subsequent export. As sea level rises and salinity intrusions push further up estuaries, we can expect the locations of enhanced sediment accumulation to also extend to more landward marginal coves.

Acknowledgments
Hydrometric data are from USGS Water Data. The authors gratefully acknowledge support from NSF (EAR-1148244 and OCE-0926427). The authors thank Kenneth Burch and Matthew Bejtlich of UMass Dartmouth for assistance with AUV deployment. Observational data from moored instruments will be made available through the ScholarWorks@Umass Amherst platform.

References

Barker, E. T., H. B. Milburn, and D. A. Tennant (1988), Field assessment of sediment trap efficiency under varying flow conditions, *J. Mar. Res.*, *46*, 573–592, doi:10.1357/002224088785113522.

Bostock, H. C., B. P. Brooke, D. A. Ryan, G. Hancock, T. Pietsch, R. Packett, and K. Harle (2007), Holocene and modern sediment storage in the subtropical macrotidal Fitzroy River estuary, Southeast Queensland, Australia, *Sediment. Geol.*, *201*(3), 321–340.

Butman, C. (1986), Sediment trap biases in turbulent flows: Results from a laboratory flume study, *J. Mar. Res.*, *44*, 645–693, doi:10.1357/002224086788403051.

Chen, C., H. Liu, and R. C. Beardsley (2003), An unstructured grid, finite-volume, three-dimensional, primitive equations ocean model: Application to coastal ocean and estuaries, *J. Atmos. Oceanic Technol.*, *20*(1), 159–186.

Festa, J. F., and D. V. Hansen (1978), Turbidity maxima in partially mixed estuaries: A two-dimensional numerical model, *Estuarine Coastal Mar. Sci.*, *7*(4), 347–359, doi:10.1016/0302-3524(78)90087-7.

FitzGerald, D. M., I. V. Buynevich, R. A. Davis, and M. S. Fenster (2002), New England tidal inlets with special reference to riverine-associated inlet systems, *Geomorphology*, *48*(1–3), 179–208, doi:10.1016/S0169-555X(02)00181-2.

Galler, J. J., and M. A. Allison (2008), Estuarine controls on fine-grained sediment storage in the Lower Mississippi and Atchafalaya Rivers, *Geol. Soc. Am. Bull.*, *120*(3–4), 386–398, doi:10.1130/B26060.1.

Gelfenbaum, G. (1983), Suspended-sediment response to semidiurnal and fortnightly tidal variations in a mesotidal estuary: Columbia River, USA, *Mar. Geol.*, *52*(1–2), 39–57.

Geyer, W. R. (1993), The importance of suppression of turbulence by stratification on the estuarine turbidity maximum, *Estuaries*, *16*(1), 113–125, doi:10.2307/1352769.

Geyer, W. R., and G. C. Kineke (1995), Observations of currents and water properties in the Amazon frontal zone, *J. Geophys. Res.*, *100*(C2), 2321–2339, doi:10.1029/94JC02657.

Geyer, W. R., J. D. Woodruff, and P. Traykovski (2001), Sediment transport and trapping in the Hudson River estuary, *Estuaries*, *24*(5), 670–679, doi:10.2307/1352875.

Grabemann, I., and G. Krause (1989), Transport processes of suspended matter derived from time series in a tidal estuary, *J. Geophys. Res.*, *94*(C10), 14,373–14,379, doi:10.1029/JC094iC10p14373.

Haines, E. B. (1976), Stable carbon isotope ratios in the biota, soils and tidal water of a Georgia salt marsh, *Estuarine Coastal Mar. Sci.*, *4*(6), 609–616.

Hansen, D. V., and M. Rattray (1965), Gravitational circulation in straits and estuaries, *J. Mar. Res.*, *23*, 104–122.

Hedges, J. I., and P. L. Parker (1976), Land-derived organic matter in surface sediments from the Gulf of Mexico, *Geochim. Cosmochim. Acta*, *40*(9), 1019–1029, doi:10.1016/0016-7037(76)90044-2.

Horne, G. S., and P. C. Patton (1989), Bedload-sediment transport through the Connecticut River estuary, *Geol. Soc. Am. Bull.*, *101*(6), 805–819, doi:10.1130/0016-7606(1989)101.

Jay, D. A., K. Leffler, H. L. Diefenderfer, and A. B. Borde (2015), Tidal-fluvial and estuarine processes in the lower Columbia River: I. Along-channel water level variations, Pacific Ocean to Bonneville Dam, *Estuaries Coasts*, *38*(2), 415–433.

Kratz, L. N. (2013), The sedimentological and geomorphological response of a glacially conditioned watershed to event induced flooding: Insights from the Connecticut River and Hurricane Irene: Amherst, MA, master's thesis, 86 pp., Univ. of Mass., University of Massachusetts. Amherst, Mass.

Kosuth, P., J. Callède, A. Laraque, N. Filizola, J. L. Guyot, P. Seyler, J. M. Fritsch, and V. Guimaraes (2009), Sea-tide effects on flows in the lower reaches of the Amazon River, *Hydrol. Processes*, *23*(22), 3141–3150, doi:10.1002/hyp.7387.

Lamb, A. L., G. P. Wilson, and M. J. Leng (2006), A review of coastal palaeoclimate and relative sea-level reconstructions using δ13C and C/N ratios in organic material, *Earth Sci. Rev.*, *75*(1), 29–57, doi:10.1016/j.earscirev.2005.10.003.

Magilligan, F. J., and B. E. Graber (1996), Hydroclimatological and geomorphic controls on the timing and spatial variability of floods in New England, USA, *J. Hydrol.*, *178*(1), 159–180, doi:10.1016/0022-1694(95)02807-2.

Meade, R. H. (1969), Landward transport of bottom sediments of the Atlantic Coastal Plain, *J. Sediment. Petrol.*, *39*, 222–234.

Milliman, J. D. (1980), Sedimentation in the Fraser River and its estuary, southwestern British Columbia (Canada), *Estuarine Coastal Mar. Sci.*, *10*(6), 609–633, doi:10.1016/S0302-3524(80)80092-2.

Milliman, J. D., and K. L. Farnsworth (2011), *River Discharge to the Coastal Ocean: A Global Synthesis*, 392 pp., Cambridge Univ. Press, Cambridge, U. K.

Milliman, J. D., and R. H. Meade (1983), World-wide delivery of river sediment to the oceans, *J. Geol.*, *91*(1), 1–21.

Monismith, S. G., W. Kimmerer, J. R. Burau, and M. T. Stacey (2002), Structure and flow-induced variability of the subtidal salinity field in Northern San Francisco Bay, *J. Phys. Oceanogr.*, *32*(11), 3003–3019.

NOAA (2016), *Tides and Currents*. [Available at http://tidesandcurrents.noaa.gov/sltrends/sltrends.html.]

Nowacki, D. J., A. S. Ogston, C. A. Nittrouer, A. T. Fricke, and P. D. T. Van (2015), Sediment dynamics in the lower Mekong River: Transition from tidal river to estuary, *J. Geophys. Res. Oceans*, *120*, 6363–6383, doi:10.1002/2015JC010754.

Odum, W. E. (1988), Comparative ecology of tidal freshwater and salt marshes, *Annu. Rev. Ecol. Syst.*, *19*, 147–176.

Olsen, C. R., I. L. Larsen, P. D. Lowry, N. H. Cutshall, and M. M. Nichols (1986), Geochemistry and deposition of ^{7}Be in river-estuarine and coastal waters, *J. Geophys. Res.*, *91*(C1), 896–908, doi:10.1029/JC091iC01p00896.

Palinkas, C. M., C. A. Nittrouer, R. A. Wheatcroft, and L. Langone (2005), The use of ^{7}Be to identify event and seasonal sedimentation near the Po River delta, Adriatic Sea, *Mar. Geol.*, *222*, 95–112, doi:10.1016/j.margeo.2005.06.011.

Parris, A. S., P. R. Bierman, A. J. Noren, M. A. Prins, and A. Lini (2009), Holocene paleostorms identified by particle size signatures in lake sediments from the northeastern United States, *J. Paleolimnol.*, *43*(1), 29–49, doi:10.1007/s10933-009-9311-1.

Patton, P. C., and G. S. Horne (1992), Response of the Connecticut River estuary to late Holocene sea level rise, *Geomorphology*, *5*, 391–417, doi:10.1016/0169-555X(92)90015-G.

Postma, H. (1967), Sediment transport and sedimentation in the estuarine environment, in *Estuaries*, pp. 158–179, Am. Assoc. for the Adv. of Sci., Washington, D. C.

Prandle, D. (1981), Salinity intrusion in estuaries, *J. Phys. Oceanogr.*, *11*(10), 1311–1324.

Ralston, D. K., and M. T. Stacey (2007), Tidal and meteorological forcing of sediment transport in tributary mudflat channels, *Cont. Shelf Res.*, *27*(10), 1510–1527, doi:10.1016/j.csr.2007.01.010.

Ralston, D. K., W. R. Geyer, and J. C. Warner (2012), Bathymetric controls on sediment transport in the Hudson River estuary: Lateral asymmetry and frontal trapping, *J. Geophys. Res.*, *117*, C10013, doi:10.1029/2012JC008124.

Ralston, D. K., W. R. Geyer, P. A. Traykovski, and N. J. Nidzieko (2013), Effects of estuarine and fluvial processes on sediment transport over deltaic tidal flats, *Cont. Shelf Res.*, *60*, S40–S57, doi:10.1016/j.csr.2012.02.004.

Ralston, D. K., G. W. Cowles, W. R. Geyer, and R. C. Holleman (2017), Turbulent and numerical mixing in a salt wedge estuary: Dependence on grid resolution, bottom roughness, and turbulence closure, *J. Geophys. Res. Oceans*, *122*, in press, doi:10.1002/2016JC011738.

Shubel, J. R. (1968), Turbidity maximum of the northern Chesapeake Bay, *Science*, *161*, 1013–1015.

Sommerfield, C. K., C. A. Nittrouer, and C. R. Alexander (1999), ^{7}Be as a tracer of flood sedimentation on the northern California continental margin, *Cont. Shelf Res.*, *19*(3), 335–361, doi:10.1016/S0278-4343(98)00090-9.

Temmerman, S., G. Govers, S. Wartel, and P. Meire (2004), Modelling estuarine variations in tidal marsh sedimentation: Response to changing sea level and suspended sediment concentrations, *Mar. Geol.*, *212*(1), 1–19, doi:10.1016/j.margeo.2004.10.021.

Thornton, S. F., and J. McManus (1994), Application of organic carbon and nitrogen stable isotope and C/N ratios as source indicators of organic matter provenance in estuarine systems: Evidence from the Tay Estuary, Scotland, *Estuarine Coastal Shelf Sci.*, *38*(3), 219–233.

Wall, G., E. Nystrom, and S. Litten (2006), Use of an ADCP to compute suspended-sediment discharge in the tidal Hudson River, New York, *U.S. Geol. Surv. Sci. Invest. Rep.*, *2006-5055*, 16 pp.

Warner, J. C., C. R. Sherwood, R. P. Signell, C. K. Harris, and H. G. Arango (2008), Development of a three-dimensional, regional, coupled wave, current, and sediment-transport model, *Comput. Geosci.*, *34*(10), 1284–1306, doi:10.1016/j.cageo.2008.02.012.

Wellershaus, S. (1981), Turbidity maximum and mud shoaling in the Weser Estuary, *Arch. Hydrobiol.*, *92*, 161–198.

Woodruff, J. D., W. R. Geyer, C. K. Sommerfield, and N. W. Driscoll (2001), Seasonal variation of sediment deposition in the Hudson River estuary, *Marine Geology*, *179*(1), 105–119, doi:10.1016/S0025-3227(01)00182-7.

Woodruff, J. D., A. Martini, E. Elzidani, T. Naughton, D. Kekacs, and D. G. MacDonald (2013), Off-river waterbodies on tidal rivers: Human impact on rates of infilling and the accumulation of pollutants, *Geomorphology*, *184*, 38–50, doi:10.1016/j.geomorph.2012.11.012.

Yellen, B., J. D. Woodruff, L. N. Kratz, S. B. Mabee, J. Morrison, and A. M. Martini (2014), Source, conveyance and fate of suspended sediments following Hurricane Irene. New England, USA, *Geomorphology*, *226*, 124–134, doi:10.1016/j.geomorph.2014.07.028.

Yellen, B., J. D. Woodruff, T. L. Cook, and R. M. Newton (2016), Historically unprecedented erosion from Tropical Storm Irene due to high antecedent precipitation, *Earth Surf. Processes Landforms*, *41*, 677–684, doi:10.1002/esp.3896.